5-2016

The Utilization of EXONEST in Characterizing Kepler Objects

Nicole Wallack
University at Albany, State University of New York

The Utilization of EXONEST in Characterizing Kepler Objects

Nicole Wallack

Honors College

Department of Physics

University at Albany

Received _____; accepted _____

Abstract

With the first detection of an exoplanet, came the study of methods to detect and characterize additional planets. Multiple methods for finding exoplanets were developed, including transit methods. When a star's flux is being observed for an extended period of time and a slight dip in the relative flux is seen periodically, this may be evidence of a planet passing in front of the star and blocking out a portion of the received flux. It is this method that is employed by the Kepler spacecraft. Kepler observes approximately 100,000 stars looking for periodic decreases in stellar fluxes. From the produced light curves, it is possible to determine characteristics of a detected planet. From these light curves, paired with different photometric properties inherent in planetary systems, much in the way of the system's nature (such as physical parameters of the planet and star and properties relating to the orbit of the planet) can be gleaned. Using the Bayesian nested sampling algorithm EXONEST, three planetary candidates observed by Kepler were studied and their characteristics determined. Due to the Bayesian nature of EXONEST, the probability of different photometric properties being present in a planetary system could be determined and compared.

Subject headings: planets and satellites: detection - methods: statistical - techniques: photometric

1. Introduction

When planets outside of our solar system, or exoplanets, were first detected, it opened humanity up to the possibility that there could be life in the planets hidden among the stars. The first discovery of a planet orbiting a sun-like star (51 Pegasi b) in 1995 launched a new era for planetary science and astronomy (Mayor & Queloz, 1995; Jenkins & Doyle, 2003). An era in which we would try to detect and characterize planets in the hopes of finding one similar to our own.

The search for planets branched into different methods of detection. These methods include radial velocity measurements, transit timing variations, and the transit method. Here, we will use light curves obtained by the Kepler Mission, which detects planets using the transit method in order to be able to monitor thousands of stars at once.

1.1. The Kepler Mission and Planetary Transits

The Kepler spacecraft was first launched in March of 2009, with the goal of finding Earth-sized planets. This 4.7 m by 2.7 m spacecraft is equipped with a photometer that is comprised of 42 charge coupled devices (CCDs), each of which has 2200 x 1024 pixels (Van Cleve et al., 2016). Using these CCDs, simultaneous high precision photometry of approximately 100,000 main-sequence stars can be done, where each pixel is recording the flux of an individual star (Borucki et al., 2003). It is through this method that the long-term luminosity of individual stars can be determined. Once the long-term luminosity of a star is determined, any changes in the brightness of a star can be observed from the normalized light curve (a plot of the relative flux, normalized to one versus time). Minute changes in the flux of a star can be due to the presence of an object in front of our line of sight of the star, which in effect, blocks a small percentage of the light from reaching, and being recorded by, the photometer.

The small changes in the apparent brightness of the star can be due to the presence of a planet blocking the light from the star before it reaches the photometer, thus producing a dip in the light curve (as shown in Figure 1). If the dip in the light curve is due to the presence of a planet, the same dip will appear periodically, with the time between dips being due to the orbit of the planet. The size and shape of the dip can indicate properties of the planet, with the depth of the dip being related to the size of the planet and the duration of the dip being how long the planet is transiting the front (with respect to Kepler) of the star. The depth of the dip is related to the size of the planet due to the fact that bigger planets will block more of the starlight when compared to smaller planets transiting the same star. When planets are detected via the transit method, the orbital inclination, planetary radius, and planetary mass (with a sin(I) degeneracy) can be estimated (Aigrain & Irwin, 2004). The transit method allows for a large number of targets to be observed simultaneously. The large number of targets inherent to the method employed by Kepler is needed because of the requirements for line of sight (Aigrain & Irwin, 2004). In order to actually observe the transit, the planet must pass between the detector and the star.

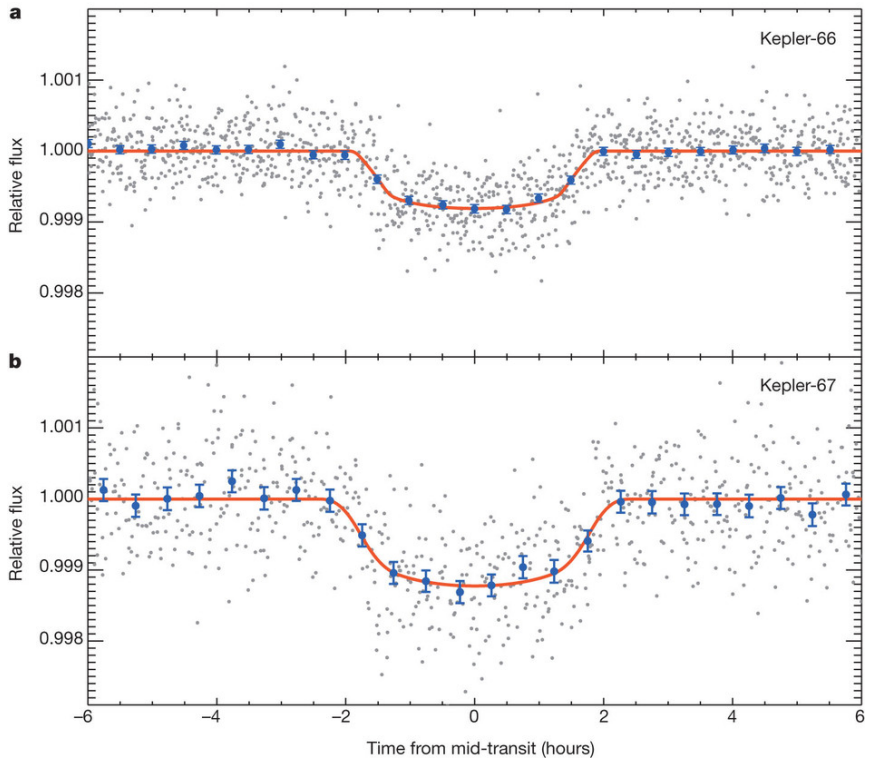

Fig. 1.— Light curves of Kepler-66 and Kepler-67 from Meibom et al. (2013). The flux of the star is normalized to one and the small dip in the light curve is due to the planetary transit.

When the planet passes behind the star, there will also be a dip in the light curve (Deming et al., 2005). A planet will reflect light from the star, which will be a part of the light curve. However, when the planet passes behind the star, the star blocks a portion of the light that would be received by the photometer onboard Kepler. This secondary planetary transit will also cause a dip in the light curve (as shown in Figure 2).

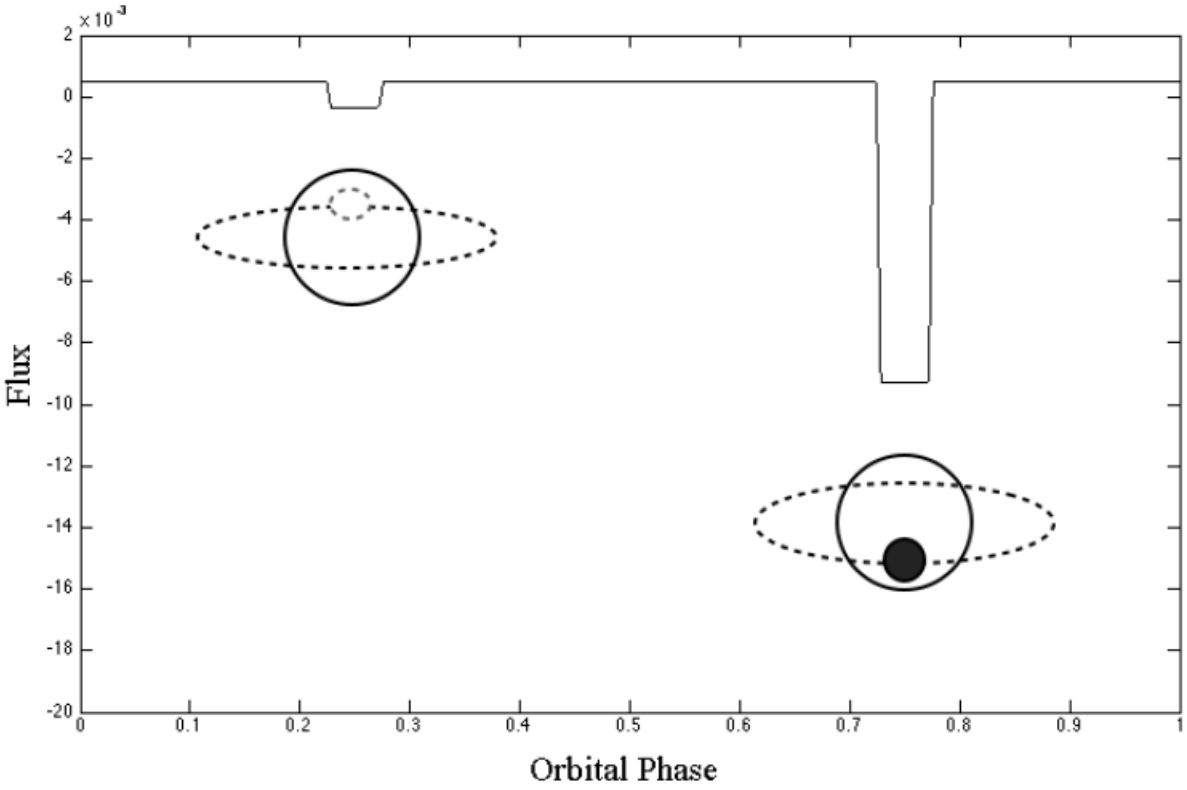

Fig. 2.— A model of a light curve with a secondary and primary transit from Placek (2014). The primary transit is shown on the right of the curve and the secondary transit is on the left side of the curve.

1.2. Photometric Effects

When analyzing a light curve, there are photometric effects which can be present and could be used to determine additional information about the planet. The four primary photometric effects are reflected light, thermal emission, Doppler beaming, and ellipsoidal variations.

Reflected light refers to the light from the planet's host star that is reflected off of the planet's atmosphere or surface. The amount of reflected light from the planet

differs depending on the position of the planet relative to the star. The thermal emission photometric effect is due to the temperature of the planet. Variations in the thermal emission would be due to differences between the dayside and nightside temperatures of the planet.

Doppler beaming is a relativistic Doppler effect, in which the apparent flux of the star changes contingent on the motion of the star relative to the observer due to the stellar wobble caused by the planet (Placek, 2014). When the star is moving towards an observer, the apparent flux of the star increases. When the star is moving away from an observer, the apparent flux of the star decreases. The planet orbiting the star causes ellipsoidal variations. The tidal forces of the planet on the star actually cause the star to become an ellipsoid.

2. Methods

Light curves were obtained from the NASA Exoplanet Archive (Akeson, 2013). The long cadence raw Kepler flux vs. time data obtained were first normalized. The long cadences were generally used because, despite the possibility of an increase in uncertainty due to not using the shorter cadences, the shorter cadences typically did produce more noise than the longer cadences. The normalization then removed any long-term trends in the data. The normalized light curves were then phase-folded so that the light curve was folded onto the most likely period of the planet (as determined by the NASA Exoplanet Archive). The normalized and phase-folded light curves were then binned. Using these reduced phase curves, characteristics of the planets were ascertained using EXONEST. In order to run EXONEST, the radius of the host star, mass of the host star, the effective temperature of the host star, the metallicity of the host star, the logarithm of the gravity of the host star, and the associated uncertainties were required. These values were obtained

from exoplanets.org and the NASA Exoplanet Archive data. Additionally, the quadratic limb darkening, linear limb darkening, and gravity darkening coefficients were needed by EXONEST and were calculated. The inclination of the orbit of the planet, the mass of the planet, and the radius of the planet were determined using a Bayesian nested sampling algorithm called EXONEST developed by Placek, Knuth, & Angerhausen (2014).

Nested sampling is used when analytical methods for doing Bayesian calculations are not possible or are inadequate. Nested sampling uses Markov Chain Monte Carlo methods to determine the sorted likelihood using randomly chosen samples with respect to the prior. The randomly sampled objects are subject to the constraint that the likelihood cannot go below the current value of the sorted likelihood function. Nested sampling iterates over the prior probability space by restricting the priors to the minimum probability found during each iteration. Threshold probabilities are assigned if the model has a higher likelihood than the previous step in the Markov Chain. The next iteration will only be accepted if the probability is greater than the threshold probability. Therefore, the limiting value of the likelihood changes as the algorithm iterates, theoretically converging on the most optimum model. Nested sampling will terminate the iterations when the user decides that most of the evidence has been found. (Sivia & Skilling, 2016)

EXONEST employs this nested sampling and Bayesian inference to estimate the values of different parameters of planetary systems including the aforementioned photometric effects (Placek, 2014). The Bayesian priors were kept constant between runs and were assigned as in Placek, Knuth, & Angerhausen (2014).

By employing the aforementioned Bayesian nested sampling algorithm, it is possible to compare the relative likelihood of different models fitting the data. In the EXONEST algorithm, different photometric effects can be turned on or off and the model can be run so that different effects are present. Each model run with different photometric effects taken into account also produces a logarithm of the evidence. These evidence values can be

compared among models run with different photometric effects so that the most probable photometric effects can be determined for an individual system.

3. Results

The light curves for Kepler-428b, Kepler-77b, and Kepler-12b were obtained from the NASA Exoplanet Archive. These three planets were selected due to their relatively small eccentricities. The planets with small eccentricities were chosen so that circular models could be run on the phase curves. The circular models were shown to both give more accurate results and converge faster than the eccentric models. The reduced phase curves were then run though EXONEST. Two different circular models were run, both with thermal variations (Circular) and without (Circular 2) in an attempt to determine whether thermal variations were present for the planetary system. The two sets of circular models could be compared using the logarithm of the evidence provided by the models. Each of the models were run for 500 samples and a 10^{-5} tolerance.

The raw flux vs. time curve (light curve) for Kepler-428b (as shown in Figure 3) was normalized, plotted as a phase curve, and binned (as shown in Figure 4).

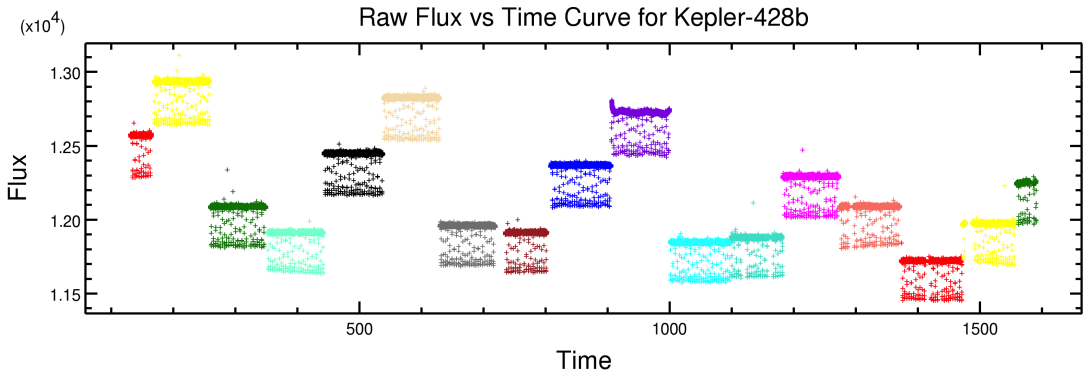

Fig. 3.— The raw light curve for Kepler-428b.

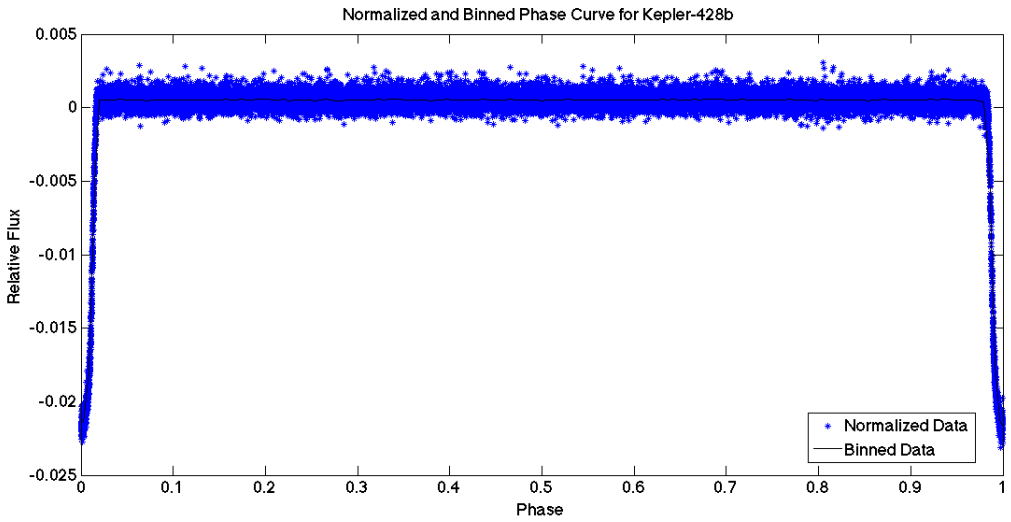

Fig. 4.— The normalized and binned phase curve for Kepler-428b.

The EXONEST algorithm was then used to fit the phase curve for the circular model with thermal variations included (shown in Figure 5) and without the thermal variations (shown in Figure 6) for Kepler-428b.

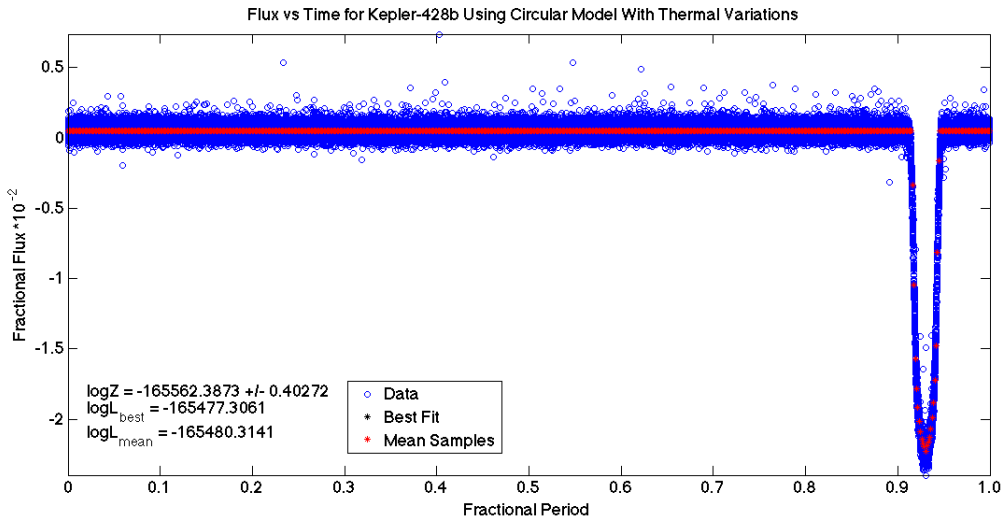

Fig. 5.— The fitted phase curve for the circular model with thermal variations with the mean samples plotted in red, the best fit in black, and the data in blue. The best fit and the mean samples overlap at all points for Kepler-428b.

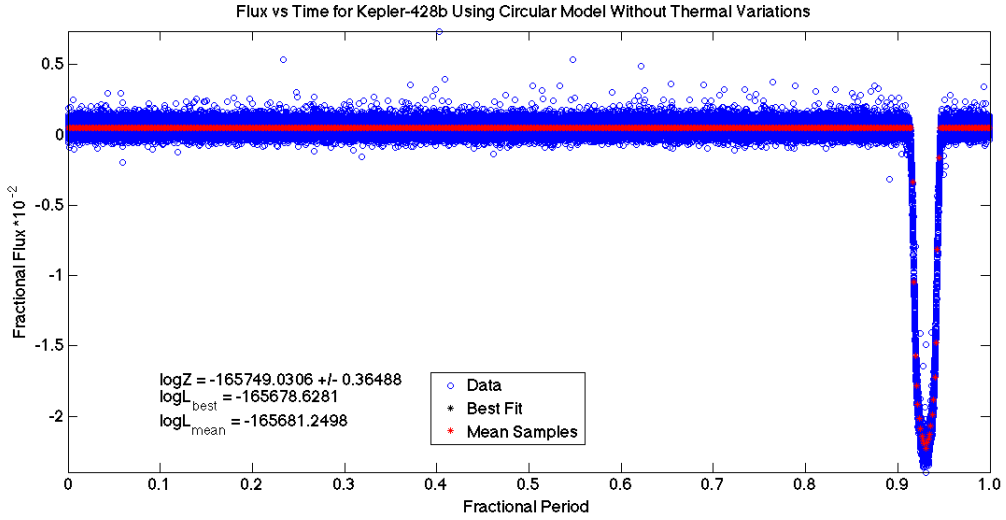

Fig. 6.— The fitted phase curve for the circular model without thermal variations with the mean samples plotted in red, the best fit in black, and the data in blue. The best fit and the mean samples overlap at all points for Kepler-428b.

The values for the planetary mass, the planetary radius, and the inclination obtained by EXONEST were compared to the values given by the NASA Exoplanet Archive (as shown in Table 1). The values for the inclination and the planetary radius were in agreement, within uncertainty, of the values given by the NASA Exoplanet Archive. However, the values for the planetary mass were not within uncertainty of the value given by the NASA Exoplanet Archive. This disagreement is likely due to the eccentricity of the orbit of Kepler-428b. The eccentricity of the orbit is given as less than 0.22, which is possibly large enough for the circular model to not be able to accurately determine the planetary mass, but still provide accurate values for the inclination and the planetary radius. The Circular and Circular 2 models both agreed with each other for the values of the inclination, planetary mass, and planetary radius. The logarithm of the evidence values were relatively close to each other (-165562.3873 and -165749.0306 for the Circular and Circular 2 models respectively), indicating that one model does not greatly fit the data better than the other.

Kepler-428b Parameters

Property	Kepler Accepted Value	EXONEST Circular Value	EXONEST Circular 2 Value
Inclination	$89.36° \pm 0.43°$	$89.1565° \pm 0.001°$	$89.1566° \pm 0.001°$
Planetary Mass	$1.27 M_{♃} \pm 0.19\ M_{♃}$	$4.2514 M_{♃} \pm 0.1532 M_{♃}$	$4.6919 M_{♃} \pm 0.1872 M_{♃}$
Planetary Radius	$1.08 R_{♃} \pm 0.03\ R_{♃}$	$1.0674 \pm 3.6483 * 10^{-5}\ R_{♃}$	$1.0675 \pm 4.7606 * 10^{-5}\ R_{♃}$

Table 1: The chart above shows the accepted values for the planetary radius, planetary mass, and inclination of Kepler-428b, as well as the values obtained by EXONEST for the Circular and Circular 2 models.

The raw light curve for Kepler-77b (as shown in Figure 7) was normalized, then plotted as a phase curve and binned (as shown in Figure 8).

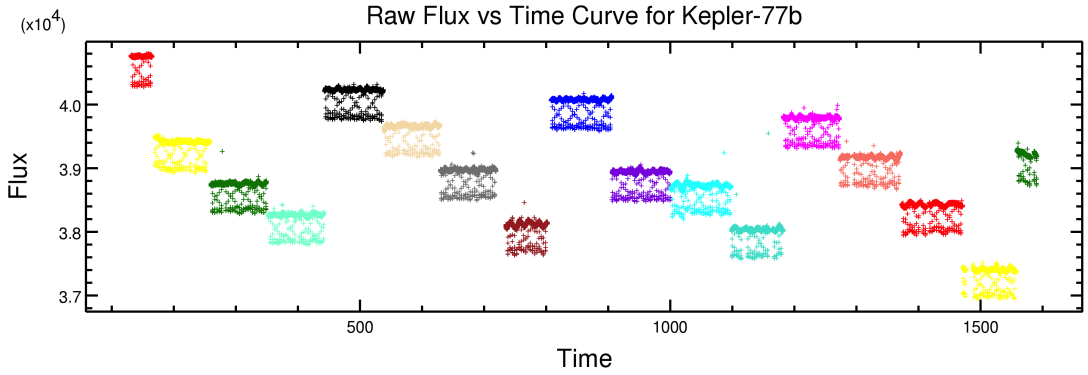

Fig. 7.— The raw light curve for Kepler-77b.

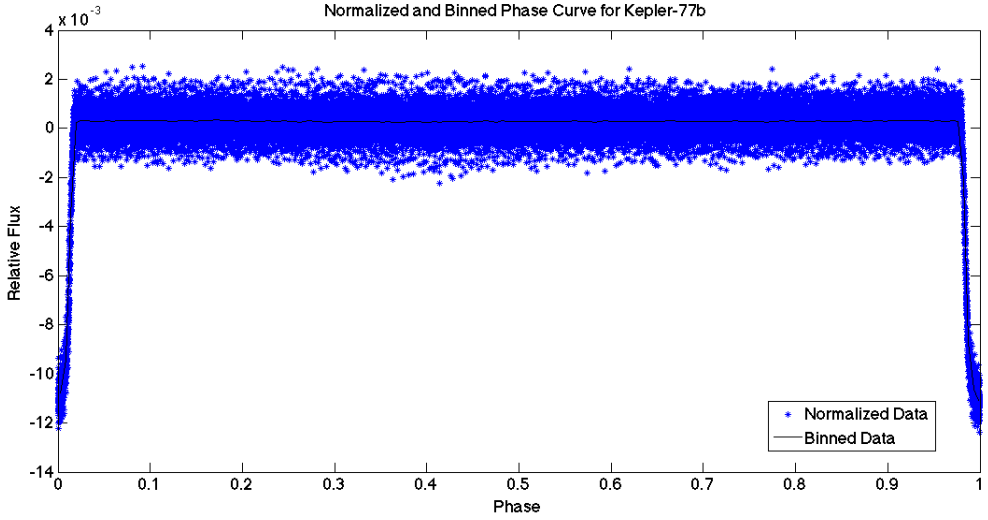

Fig. 8.— The normalized and binned phase curve for Kepler-77b.

The EXONEST algorithm was then used to fit the phase curve for the Circular model (shown in Figure 9) and Circular 2 model (shown in Figure 10) for Kepler-77b.

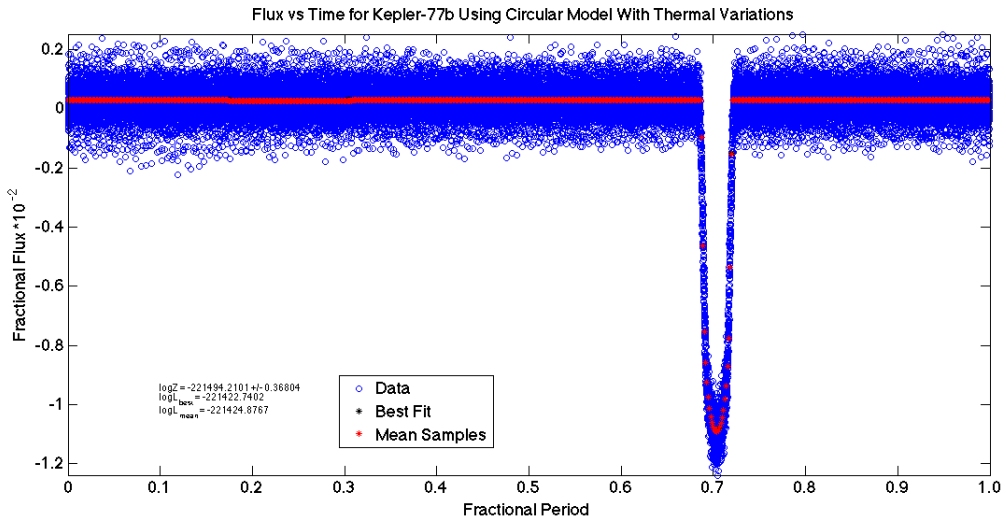

Fig. 9.— The fitted phase curve for the circular model with thermal variations with the mean samples plotted in red, the best fit in black, and the data in blue. The best fit and the mean samples overlap at all points for Kepler-77b.

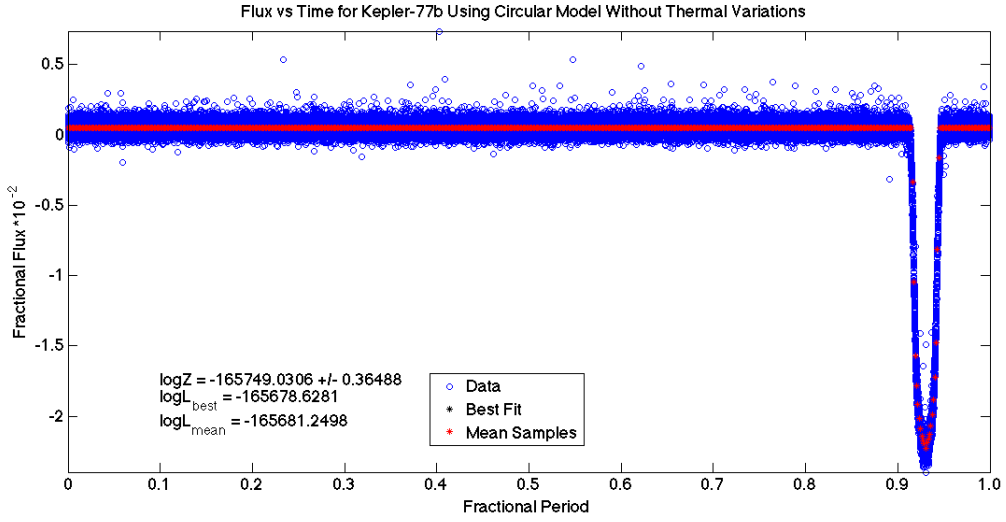

Fig. 10.— The fitted phase curve for the circular model without thermal variations with the mean samples plotted in red, the best fit in black, and the data in blue. The best fit and the mean samples overlap at all points for Kepler-77b.

The values for the planetary mass, the planetary radius, and the inclination obtained by EXONEST were then also compared to the values given by the NASA Exoplanet Archive (as shown in Table 2). The values for the planetary radius were in agreement with the values given by the NASA Exoplanet Archive. However, the value for the planetary mass and the inclination were not within uncertainty of the accepted values. Both calculated inclinations, while not within the uncertainty, were within 1.5 uncertainties of the value given by the NASA Exoplanet Archive. The planetary mass, on the other hand, was not nearly in agreement with the accepted value. This disagreement is not due to a high eccentricity like in the case of Kepler-428b. The eccentricity of Kepler-77b is zero as determined by the NASA Exoplanet Archive. The disagreement in Kepler-77b is likely do to the small size of the planet. EXONEST does not appear to be sensitive to detecting the mass of small (less than 1 Jupiter mass) planets. The Circular and Circular 2 models both agreed with each other for the values of the inclination, planetary mass, and planetary radius. The logarithm of the evidence values were once again relatively close to each other (-221494.2101 and -221545.9859 for the Circular and Circular 2 models respectively), indicating that one model does not greatly fit the data better than the other. However, these values of the logarithm of the evidence were much more negative than those of Kepler-428b, further indicating the lack of proper fitting of the data.

Kepler-77b Parameters

Property	Kepler Accepted Value	EXONEST Circular Value	EXONEST Circular 2 Value
Inclination	$88.00° \pm 0.11°$	$88.1547° \pm 0.001°$	$88.1505° \pm 0.001°$
Planetary Mass	$0.430 M_{♃} \pm 0.032\ M_{♃}$	$2.4897 M_{♃} \pm 0.2188 M_{♃}$	$2.555 M_{♃} \pm 0.2300 M_{♃}$
Planetary Radius	$0.960 R_{♃} \pm 0.016\ R_{♃}$	$0.9483 \pm 0.0001051\ R_{♃}$	$0.9481 \pm 0.0001020\ R_{♃}$

Table 2: The chart above shows the accepted values for the planetary radius, planetary mass, and inclination of Kepler-77b, as well as the values obtained by EXONEST for the Circular and Circular 2 models.

The raw flux vs. time curve for Kepler-12b (as shown in Figure 11) was then normalized, plotted as a phase curve, and binned (as shown in Figure 12).

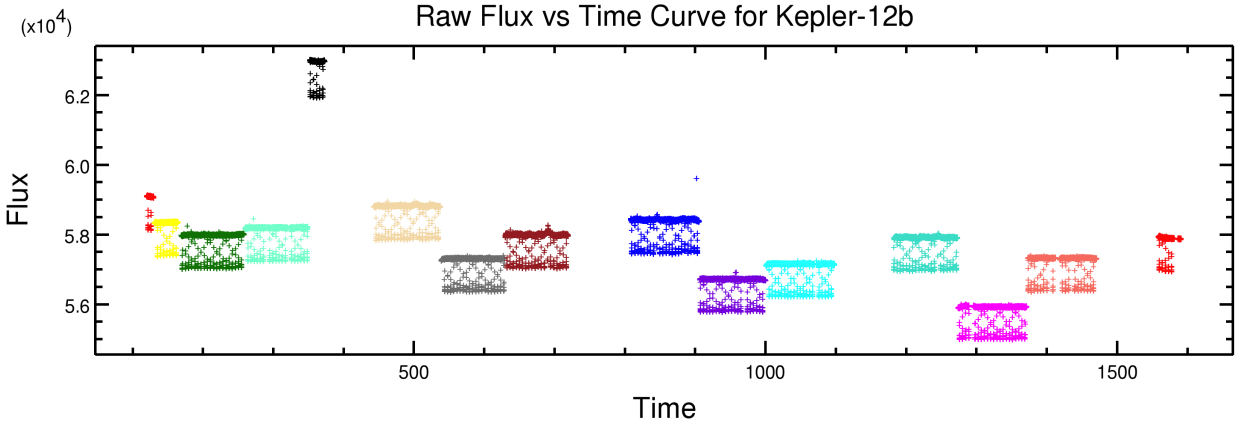

Fig. 11.— The raw light curve for Kepler-12b.

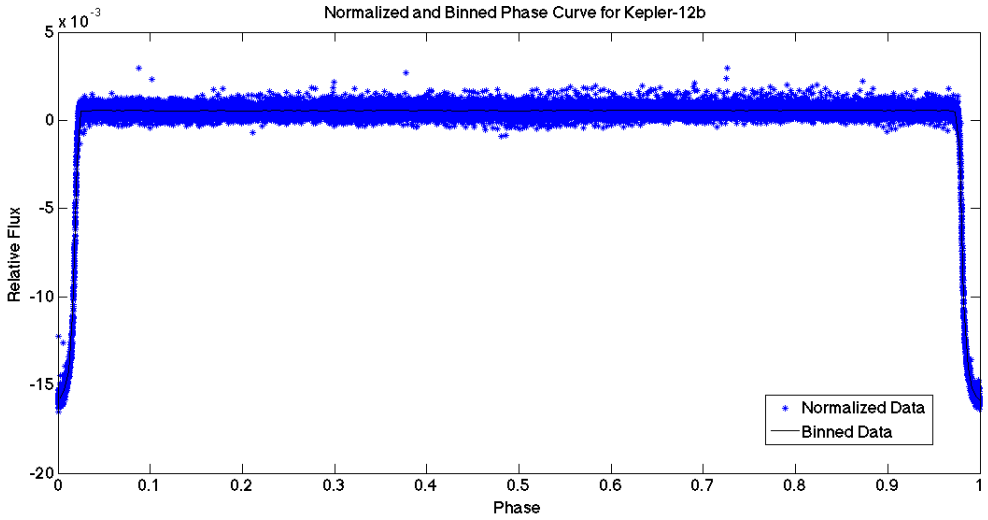

Fig. 12.— The normalized and binned phase curve for Kepler-12b.

The EXONEST algorithm was then used to fit the phase curve for the Circular model (shown in Figure 13) and Circular 2 model (shown in Figure 14) for Kepler-12b.

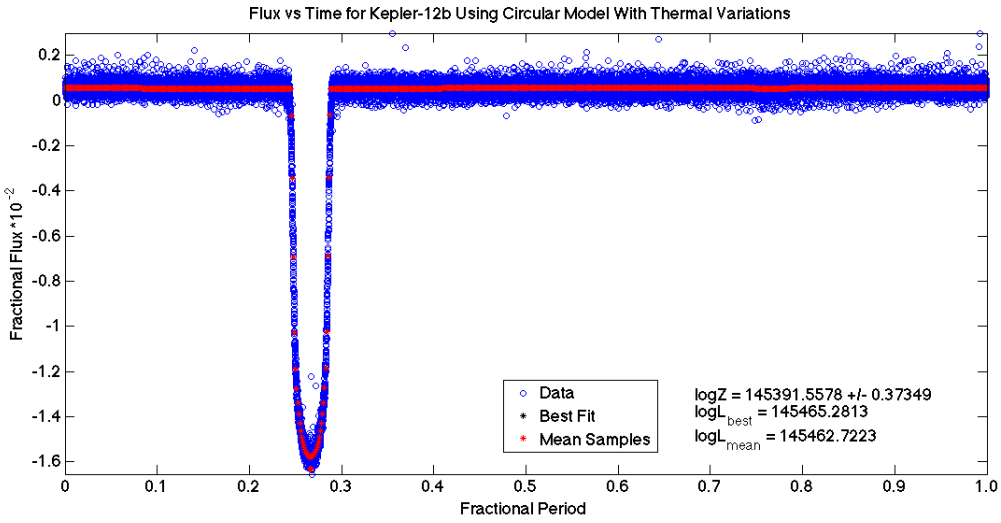

Fig. 13.— The fitted phase curve for the circular model with thermal variations with the mean samples plotted in red, the best fit in black, and the data in blue. The best fit and the mean samples overlap at all points for Kepler-12b.

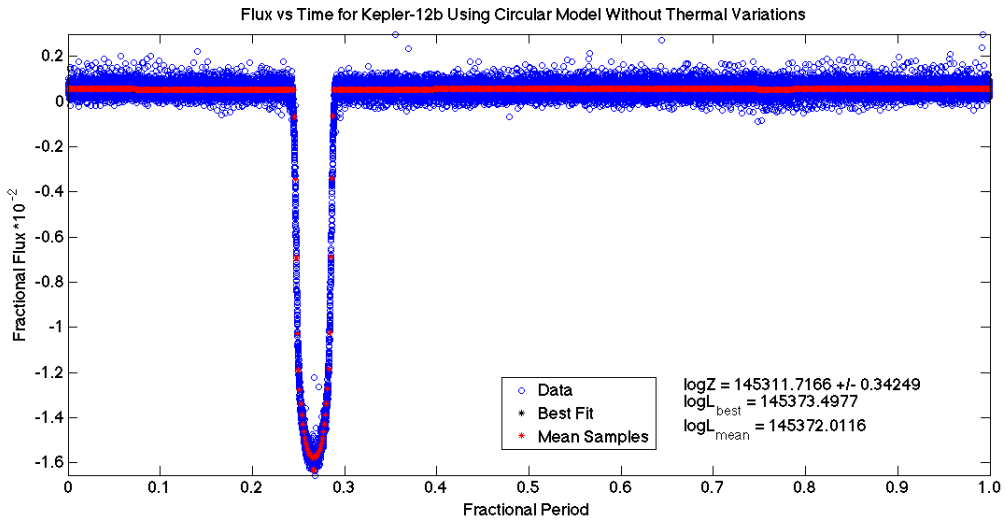

Fig. 14.— The fitted phase curve for the circular model without thermal variations with the mean samples plotted in red, the best fit in black, and the data in blue. The best fit and the mean samples overlap at all points for Kepler-12b.

The values for the planetary mass, the planetary radius, and the inclination obtained by EXONEST were then also compared to the values given by the NASA Exoplanet Archive (as shown in Table 3). The values for the planetary radius were in agreement with the values given by the NASA Exoplanet Archive. However, the values for the planetary mass and the inclination were not within uncertainty of the values given by the NASA Exoplanet Archive. Both calculated inclinations, while not within the uncertainty, were also within 1.5 uncertainties of the value given by the NASA Exoplanet Archive. The planetary mass, like Kepler-428b and Kepler-77b, was not nearly in agreement with the accepted value. This disagreement might be due to the eccentricity, since the eccentricity was not listed by the NASA Exoplanet Archive. Similarly to Kepler-77b, the disagreement in the values could also be due to the small size of the planet. This reinforces the likelihood that EXONEST is not sensitive to small planets. The Circular and Circular 2 models both agreed with each other for the values of the inclination, planetary mass, and planetary

radius. The logarithm of the evidence values were once again relatively close to each other (145391.5578 and 145311.7166 for the Circular and Circular 2 models respectively), indicating that one model does not greatly fit the data better than the other.

Kepler-12b Parameters

Property	Kepler Accepted Value	EXONEST Circular Value	EXONEST Circular 2 Value
Inclination	$88.796°^{+0.088°}_{-0.074°}$	$88.6935° \pm 0.001°$	$88.6945° \pm 0.001°$
Planetary Mass	$0.432^{+0.053}_{-0.051}\ M_{♃}$	$2.7621 M_{♃} \pm 0.2139\ M_{♃}$	$3.8168 M_{♃} \pm 0.20447 M_{♃}$
Planetary Radius	$1.754^{+0.031}_{-0.036}\ R_{♃}$	$1.7239 \pm 0.0001257\ R_{♃}$	$1.724 \pm 0.000142\ R_{♃}$

Table 3: The chart above shows the accepted values for the planetary radius, planetary mass, and inclination of Kepler-12b, as well as the values obtained by EXONEST for the Circular and Circular 2 models.

In all three cases, EXONEST was not able to ascertain the mass of the planet. In all three cases, the values determined for the planets' radii were in agreement with the values determined by the NASA Exoplanet Archive. The inclination in all three cases, were within 1.5 uncertainties of the values given by the NASA Exoplanet Archive.

4. Conclusions and Discussion

Ever since the first exoplanet was discovered more than twenty years ago, there have been pursuits to detect and characterize exoplanets. There have been numerous methods that have been enacted to try to find these other worlds. One of the most popular methods is the transit method, which is employed by the Kepler spacecraft. The transit method involves observing a star for an extended period of time in order to be able to characterize its flux over time. In this way, minute changes in the stellar flux, possibly due to a planet

passing between the line of sight and the star, can be found. These light curves can be used to determine properties about not only the star, but also the possible planet that it hosts.

Three planets, Kepler-428b, Kepler-77b, and Kepler-12b were analyzed using the nested sampling algorithm EXONEST. Using EXONEST, it is possible to determine the inclination, planetary mass, and planetary radius of a system. Two different circular models were tested (one without thermal variations and one with thermal variations) and the values ascertained by the models were compared to the accepted values published by the Exoplanet Data Archive. Both models were generally in agreement with each other as to the values of the planetary properties, indicating the relative unimportance of thermal variations in these systems.

In all three planets, the values calculated for the planetary radius were within uncertainty of the accepted values. The values calculated for the inclination were not within uncertainty for two of the planets, namely Kepler-77b and Kepler-12b, but were within 1.5 uncertainties of their respective accepted values, pointing to the relative accuracy of EXONEST in determining the inclination. The planetary masses proved to be the least in agreement with the accepted values, deviating as much as an order of magnitude for Kepler-77b and Kepler-12b. The lack of agreement among all of the modeled masses and the accepted values could be do to the eccentricities of the systems being too high to accurately be modeled by a circular system (possibly the case in Kepler-428b), the small size of the planets (possibly in the cases of Kepler-77b and Kepler-12b), or possibly due to the activity of the star affecting the light curve. Another possibility relates to the nature of the data that was used. Only the long cadences of the planets were used with EXONEST, which possibly could have resulted in errors in the calculated properties.

A further study could explore the sensitivity of EXONEST as it pertains to the mass of the planet. It appears from this cursory study that the smaller the planet, the bigger the

difference between the expected and calculated masses. In the case of Kepler-428b, a planet with a mass greater than that of Jupiter, EXONEST was able to get within an order of magnitude of the correct value, whereas in the cases of the sub-Jovian Kepler-77b and Kepler-12b, EXONEST was greater than an order of magnitude off in its calculation of the mass. Although being within an order of magnitude is not accurate enough to actually make a determination as to the planetary mass, it does, when compared to the higher inaccuracy of the masses determined for the smaller planets, point towards a possible mass and accuracy relationship. Therefore, a sensitivity study would be a beneficial further endeavor.

Sincerest thanks to Professor Knuth for his guidance in this work and for his advisement over the course of my undergraduate career. If not for Professor Knuth's unwavering support, I would not have been able to have completed this work nor reached my goal of being able to attend graduate school in the fall. Also deserving of thanks is the entirety of the Department of Physics, which has served as a support network over the past four years.

REFERENCES

Aigrain, S.& Irwin, W. 2004, "Practical Planet Prospecting" MNRAS 350, 331-345

Akeson, R.L., Chen, X., Ciardi, D., et al., 2013, "The NASA Exoplanet Archive: Data and Tools for Exoplanet Research" PASP 125:989-999

Borucki, W.J., Koch, D.G., Lissauer, J.J., et al. 2003, "The Kepler Mission: a Wide-Field-of-View Photometer Designed to Determine the Frequency of Earth-Size Planets Around Solar-Like Stars" Proceedings of the SPIE. 4854, 129-140

Deming, D., Seager, S., Richardson, L. J., & Harrington, J. 2005, "Infrared Radiation from an Extrasolar Planet" Nature 434, 740

Jenkins, J.M. & Doyle, L.R., 2003, "Detecting Reflected Light From Close-In Extrasolar Giant Planets With The Kepler Photometer" ApJ 595:429445

Mayor, M. & Queloz, D. 1995, "A Jupiter-mass companion to a solar-type star" Nature 378, 355-359

Meibom, S., Torres, G., Fressin, F., et al. 2013, "The same frequency of planets inside and outside open clusters of stars" Nature 499, 5558

Placek, B. 2014,"Bayesian Detection and Characterization of Extra-Solar Planets Via Photometric Variations" ProQuest Dissertations And Theses.

Placek, B., Knuth, K., & Angerhausen, D. 2014"EXONEST:Bayesian Model Selection Applied to the Detection and Characterization of Exoplanets Via Photometric Variations" ApJ 795:112-127

Sivia, D., & Skilling, J. 2006, "Data Analysis: A Bayesian Tutorial" (Oxford: Oxford Univ. Press)

Van Cleve, J., Caldwell, D., Haas, M.R., Howell, S.B. 2016, "Kepler: A Search for Terrestrial Planets" STSCI

This manuscript was prepared with the AAS LaTeX macros v5.2.